

## Effects of the Velocity and the Nature of the Inert Gas on the Stainless Steel Laser Cut Quality

S. Aggoune<sup>1</sup>, E.H. Amara<sup>1</sup> and M. Debiane<sup>2</sup>

**Abstract:** The effects of inert assisting gas nature and velocity on laser cut quality are investigated. A pure fusion cutting process just above melting point is considered, where the molten steel velocity is given as a function of the two acting forces represented by the pressure gradient and the frictional forces applied by the laminar gas flow. In the case of nitrogen assisting gas, the stainless steel melt film exhibits a visible separation point. The point where the melt flow is separated out from the solid wall depends strongly on the gas velocity. It is pushed down the cut surface when the gas velocity is increased. Furthermore, we have investigated the use of different inert gases (nitrogen, argon and helium) to blow the molten material out of the kerf, and it was noted that the argon and the nitrogen gases evacuate more easily the molten metallic film, compared to the helium gas from their cooling rates point of view. It is concluded that the two first gases are more efficient in laser cutting process of metals. We have studied a 4 mm stainless steel plate thickness without taking into account the transverse movement of the treated workpiece, the numerical solution is obtained by the volume of fluid (VOF) and solidification/melting models, implemented by Fluent CFD software.

**Keywords:** boundary layer, cutting, flow, fusion, gas, inert, laser, melt, metal, steel.

### 1 Introduction

Laser cutting technology involves: inert-gas fusion cutting, reactive-gas fusion cutting and vaporization cutting. This technology consists in heating a finite volume of material to melt and/or evaporate it. It is a non contact process with a high precision. Metal cutting is an important modern domain where the material is made

---

<sup>1</sup> CDTA, Laser Material Processing Team, PO. BOX 17 Baba-Hassen, 16303 Algiers, Algeria. sam-aggoune@yahoo.fr

<sup>2</sup> USTHB, Theoretical and Applied Fluid Mechanics Laboratory, PO. BOX 32 El-Alia, Algiers, Algeria

molten by a focused beam and then removed by an intense gas jet adjusted coaxially with the laser beam. The assisted gas has three effects: cooling the cut surfaces and protect the irradiated region from the high temperature oxidation reactions and blow out the molten metal from the workpiece cutting front walls [Yilbas and Sahin (1995)].

The effects of high gas pressure on high power CO<sub>2</sub> laser cutting process were examined by Chen (1999), whereas laser cutting parameters effects on the cut quality in thin-section steel has been investigated by Golnabi and Bahar (2009). The authors found that during oxygen assisted laser cutting of thin-section (< 2 mm) of stainless steel and mild steel using a Nd: YAG laser, the mild steel required a lower oxygen gas pressure than stainless steel cutting, and the kerf width in mild steel was larger than that in stainless steel.

In reactive fusion cutting, an active assist gas jet acts as another heat source in the cutting process. The oxide layer may need to be removed by a cleaning operation. Usually, oxygen or compressed air passing through the cut kerf plays another important role, namely providing additional heating to the cutting process. The supplied energy amount by the exothermic reaction varies following the material; with mild steel and stainless steel it is about 60% of the energy used for cutting, and with a reactive metal like titanium it is around 90%. Indeed, for stainless steel laser cutting, the assist gas usually used is nitrogen which gives clean cut surfaces and doesn't require any cleaning operation. Tani et al. (2003) showed that the two mechanisms responsible for dross formation are: the surface tension of the melt and the build-up of melt at the bottom resulting from an incomplete ejection of the molten material. An analytical approximation of the heat conduction losses during the cut of metals was developed by Schulz et al. (1993, 1999). They have also deduced that, a laminar boundary layer is required in order to keep a high cutting quality. The ejection of melt from the laser cut kerf is mainly driven by two forces exerted by the assist gas jet which includes: the frictional force at the gas/melt interface and the pressure gradient. Both contributions are of the same orders [Vicanek and Simon (1987)]. They also concluded that these two strengths increase with increasing velocity of the gas jet and with that of the angle of inclination of the kerf. Thick section metal cutting was studied by Beyer et al. (2008) and Hammann (2008). They argued that the poor cut quality found in thick-section metal in the case where a fibre laser is used, is due to the greater absorption of the 1  $\mu$ m radiation which involves in increased melting capacity and the poor melt ejection compared to the melting capacity and melt ejection obtained with the 10  $\mu$ m CO<sub>2</sub> laser radiation. The authors showed that an acceptable cutting quality region does not exist for pure oxygen cutting mainly because of the dross formation under the cut kerf due to the exothermic reaction. To avoid the formation of oxides, it is rec-

ommended to use an inert gas. In that case, the heat affected zone (HAZ) is small and the edges are less deformed. The work of Abdulahdi (1997) is purely based on experiment and focuses on the calculation of the HAZ, and the metallurgical transformations of steels subjected to the laser irradiation. In their contribution, Mas et al. (2003) help in the understanding of cutting process of cut of metals by laser and provides a consistent physical approach of all physical phenomena that occur when a metal sample subjected to intense laser irradiation.

The dynamic of the gas flow constitutes an important factor in the cut result quality so that considerable research studies were carried out to improve the capability of the assist gas to remove the molten material from the kerf. The problem of subsonic and supersonic gas flows through narrow channels is being studied by many authors to investigate the mechanism of laser cutting steel metal. These authors examine the instabilities and roughness generated when the operating gas is oxygen which executes an additional energy of chemical reactions. For instance, Kovalev et al. (2008) studied theoretically and experimentally the specific features of subsonic jet flows of oxygen assisting gas in a narrow and flat channel simulating the laser cut. Their study shows for low inlet pressures of the gas a large vortex located at the exit of the channel and flow oscillations near the wall. The preferred procedure to cut stainless steel is the inert-gas fusion cutting process.

This paper investigates the effect of an inert gas jet on the cut kerf quality of stainless steel workpiece. The influence of nitrogen gas velocity increasing on the separation point appearance is also studied. The behaviour of the molten material using three kinds of inert gases: nitrogen, argon and helium is analysed to deduce the appropriated gas to evacuate the molten metal easily. Fluent softwares were used for the numerical resolution of the Navier-Stokes equations.

## **2 Modelling**

During the cut, the molten metal is removed with the gas jet, there is only a thin layer of the melt that remains on the cutting front. We obtain thus a molten boundary layer. For this study we have used a narrow channel, shown in fig. 1, geometrically similar to a pattern given in laser cut.

### **2.1 Hypotheses**

To specify the problem of the molten metal flow, we assume on the liquid boundary layer:

- The thickness of the liquid film is very small compared with that of the Kerf (channel), so we can consider the ejection as a two dimensional problem.

- The slope of the front of cut is negligible.
- The conduction is dominant and the evaporation is negligible.
- The radiation and convection are neglected.
- The metallic liquid is supposed to be a laminar and viscous fluid.

For the gas flow, we suppose that:

- The gas flow is divided into a region of irrotational motion and boundary layer located at the front cutting.
- It is subsonic and laminar.

Thus we are in the presence of two superposed boundary layers with parabolic velocity profiles.

## 2.2 Laminar boundary layer equations of the molten metal

The ejection of the liquid metal is mainly driven by two forces induced by the gas jet, and acting on the melt including: the shear stress force at the interface and the pressure gradient.

The Navier-Stokes equations of the molten metal are written as follows:

$$\frac{\partial u_x}{\partial t} + \rho(u_y \frac{\partial u_x}{\partial x} + u_y \frac{\partial u_x}{\partial y}) = -\frac{\partial P}{\partial x} + \mu(\frac{\partial^2 u_x}{\partial x^2} + \frac{\partial^2 u_x}{\partial y^2}) \quad (1)$$

$$\frac{\partial u_y}{\partial t} + \rho(u_x \frac{\partial u_y}{\partial x} + u_y \frac{\partial u_y}{\partial y}) = -\frac{\partial P}{\partial y} + \frac{\partial}{\partial x}(\eta \frac{\partial u_y}{\partial x}) + \mu(\frac{\partial^2 u_y}{\partial x^2} + \frac{\partial^2 u_y}{\partial y^2})$$

Where  $u_x$  and  $u_y$  are the molten metal velocity vector components in the  $x$  and  $y$  directions respectively,  $\rho$  is the density of the metallic molten film and  $\mu$  its dynamic viscosity. On the other hand,  $\eta$  is the dynamic viscosity of the gas jet.

At a fixed time and by neglecting evaporation and convective terms near the viscous dissipation terms, the equations are reduced to:

$$\begin{aligned} -\frac{\partial P}{\partial x} &= 0 (P = P(y)) \\ 0 &= -\frac{\partial P}{\partial y} + \frac{\partial}{\partial x}(\eta \frac{\partial u_y}{\partial x}) + \mu(\frac{\partial^2 u_y}{\partial x^2}) \end{aligned} \quad (2)$$

The boundary conditions taken at the solid walls and at the interface liquid / gas can be written as follows:

$$\begin{aligned} x = 0, u_x &= 0 \\ x = \delta, \quad \eta \left. \frac{\partial u}{\partial x} \right|_{x=\delta} &= \tau \end{aligned} \quad (3)$$

So we can deduce the velocity of the molten metal as a function of the shear stress and the pressure gradient exerted by the gas jet:

$$\begin{aligned} 0 &= -\frac{\partial P}{\partial y} + (\eta + \mu) \frac{\partial^2 u_y}{\partial x^2} \quad \Rightarrow \\ u_l = u_y &= \frac{1}{(\eta + \mu)} \left( \frac{\partial P}{\partial y} \right) \left[ \frac{x^2}{2} - \delta x \right] + \frac{\tau}{\eta} x \end{aligned} \quad (4)$$

### 2.3 Numerical method and simulation

To achieve the modelling, the calculation field, the grid and the boundary conditions reservation were defined by the means of the pre-processor Gambit, whereas the computing was processed by the solver Fluent to solve numerically the Navier-Stokes equations, on the base of the finite volume method [Patankar (1980)]. Mesh refinement at the boundary layers has been performed in order to distinguish the various flow patterns at these locations characterized by high gradients of temperatures and velocities. Elsewhere the grid spacing was uniform; see fig. 1. FLUENT is a powerful tool basically for solving fluid flow equations via the finite volume method. This method consists to divide the domain into discrete volumetric elements and the physical quantities are defined in the centroid of each element. Over each element and using an interpolation function for the variable in question, the concerning conservation laws are integrated (velocity components and pressure). The obtained algebraic equations are then linearized and solved iteratively. The convergence of the iterative resolution is checked by the evolution of the individual values of every variable during the iterations. The residual in every control volume is defined as follows:  $R_\varphi = a_P \varphi_P - \sum_i a_i \varphi_i - S$

Furthermore a post-processing is started to exploit and to present the results.

With FLUENT it is possible to simulate compressible and incompressible fluids at the same time, and also multiphase flow with free surfaces. In our work the so called volume of fluid (VOF) model is best suited for the tracking of sharp interfaces. The interface between the two immiscible fluids, namely the molten stainless steel and the nitrogen gas. In this model, a volume fraction corresponding to the volumetric occupation of the regarding phase is introduced. For this Fluent

provides the so-called geometric reconstruction scheme which is a discretization scheme for the volume fraction, where the interface between two phases is always ensured to be sharp. Several elements around the physical interface would be occupied by the both phases. Within the VOF model and the geometric reconstruction scheme the surface tension must be considered.

The change state of the stainless steel from liquid to solid during the cooling induced by the ejected gas is treated by melting and solidification model. This model is implemented in FLUENT by an enthalpy based phase change approach, it includes a mushy region around the melting point, where the material is linearly changing from solid to liquid.

In this work the so-called pressure based segregated solver is used, because this is best for handling free surface flow. The momentum equation for the velocity components is solved sequentially by the algorithm; afterwards a pressure correction is calculated by solving a pressure equation to satisfy the continuity. This correction is used to update the pressure and velocity field. For this, the velocity components are stored at a location midway between the grid points, i.e. on the control volume faces. All other variables including pressure are calculated at the grid points. This arrangement handles the pressure linkages through the continuity equation and is known as Semi-Implicit Method for Pressure-Linked Equations (SIMPLE) algorithm. The details of this algorithm are given in the literature [Patankar (1980)].

During the numerical resolution of the equations by the processor FLUENT, user defined functions (UDFs) written in C programming language, extended by a library containing functions can be interactively loaded. In our case this later is used to define some physical properties of our material which depend on the temperature.

The assigned time step was  $10^{-6}$ s, it allowed to obtain a convergence of the problem, and the convergence criterion for the residuals was set as  $|\psi^k - \psi^{k-1}| \leq 10^{-6}$  to stop the simulations.

### 3 Results and discussions

In case of laminar inert assistance gas there was a tendency for the appearance of a separation point in the boundary layer of the metallic molten film. This was observed when the inertia force (Pressure gradient) was very higher compared to the viscous force (shear stress). In that situation, there is a possibility of transition from the laminar to the turbulent boundary layer of the melt flow.

In the contact of the wall, when the profile of the velocity presents an infinite slope, it is asked that there is a boundary layer separation point. After that point, the flow becomes turbulent, and so the viscous forces are not enough important: we assist

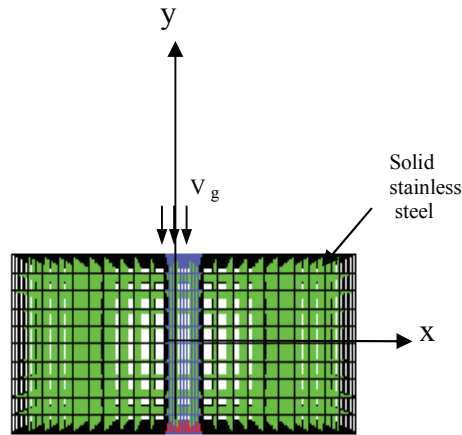


Figure 1: Mesh generated in the solution domain

then to the production of vortices which are responsible of energy dissipation.

Concretely, the transition from the laminar regime to the turbulent one is manifested by a sudden thickening of the melt boundary layer, in order to satisfy continuity within the layer. An increase of thickness of the melt layer leads to a poor quality of the cutting.

### 3.1 State of the molten metal during the ejection by a nitrogen gas

The temperature of the molten stainless steel sheared and blown away from the kerf with nitrogen gas jet is kept at the melting temperature i.e 1712 K. This layer is supposed to be already formed at the initial time of simulation and a thickness of  $100\mu\text{m}$  is supposed. The gas jet temperature at the inlet kerf (1mm width) is 300 K and its velocity is fixed to 10m/s.

As a result of the simulation, on figure 2, we show the liquid fraction distribution obtained by implementing the VOF model used in interface tracking.

On the figure we note that at the time equal to  $10^{-5}$  s the separation point did not appeared yet, but this becomes very clear at the times shown on the isocolor pictures, and corresponding to  $2 \cdot 10^{-4}$ s,  $1.2 \cdot 10^{-3}$ s and  $3 \cdot 10^{-3}$ s. The separation point is located approximately at a distance of 1.7mm from the kerf entrance. This point is followed by a resolidification of the molten metal, due to the presence of vortices produced by the transition from the laminar to the turbulent regime which cool and solidify it further.

Indeed, for the fixed value of gas velocity (10m/s), the flow of the molten metal slows down so that the viscous forces in the boundary layer become more and more

significant, this later wins in thickness:  $(du/dy)$  decreases because  $(dy)$  increases. This situation leads to lower shear stresses to drag the slow molten metal particles located near the solid wall.

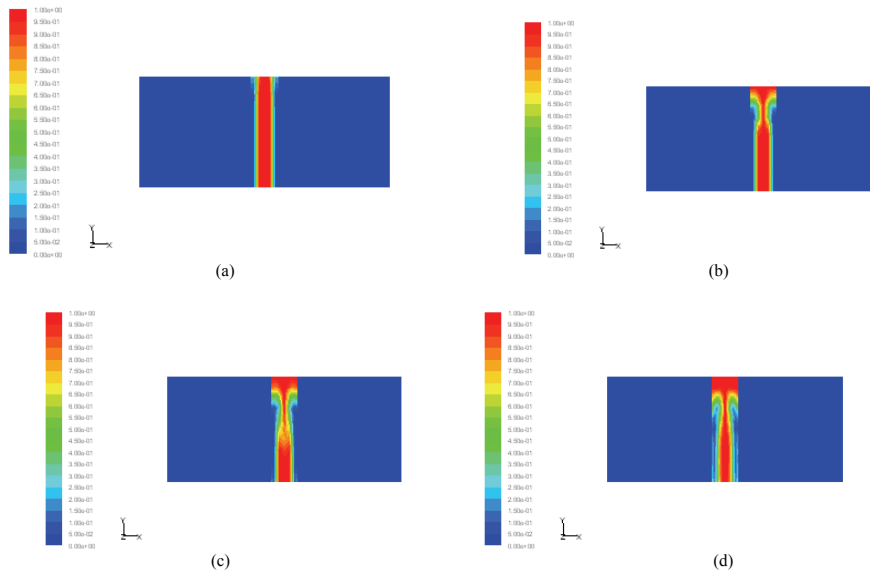


Figure 2: Molten metal state blown by a nitrogen gas taken at different times: (a)  $t=1.10^{-5}$ s, (b)  $t=2.10^{-4}$ s, (c)  $t=1.2.10^{-3}$ s and (d)  $t=3.10^{-3}$ s

After the separation point and the appearance of turbulence, the heat transfer from the metallic liquid to the stream gas is very effective; so we have a cooling of the boundary layer of the molten stainless steel. This situation leads to its solidification again, and as a result the cutting edges become thick and rough.

### 3.2 Effect of the velocity of the nitrogen gas jet on the position of the separation point

In the following, we focus on the phenomena that will occur by varying the gas assistance velocity, at a given time which is chosen equal to  $10^{-3}$ s. Figure 3 illustrates that in the case of nitrogen assisting gas, the stainless steel melt film exhibits a clear separation point which depends strongly on the gas velocity. Indeed, when the velocity of the gas jet increases from 10m/s to 40 m/s, the separation point moves downward the workpiece from 1mm to 1.7mm. This means that for cleaning and reducing the surface from roughs we have to increase the assist gas velocity. In addition, the high velocity of the nitrogen jet increases the tendency to resolidifying

the melt near the solid walls, and after the appearance of the separation point since heat transfer from the hot kerf walls to the fluid increases in this region (see fig. 3).

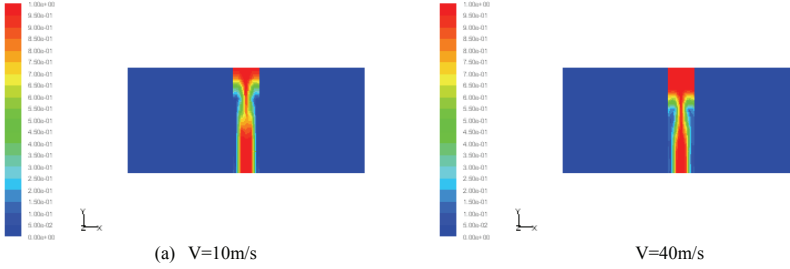


Figure 3: Separation point position for two different velocities of nitrogen gas jet.

### 3.3 Influence of various inert gases on the quality of the cutting surface

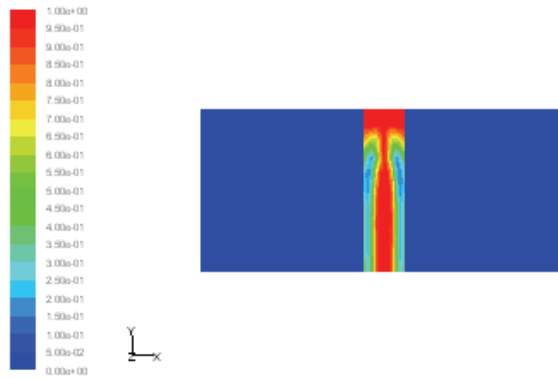
For further investigation, we have studied the effect of the assisting gas nature. Also for a given simulation time taken equal to  $3 \cdot 10^{-3}$ s, and for a velocity of the gas jet taken equal to 10 m/s, we have noted as shown on figure 4, that the separation point position varies slightly with the nature of the used gas. On the other hand the solidification of the molten stainless steel is significantly different.

By neglecting the heat generated by internal frictions and temperature rise due to the adiabatic compression, the heat transfer from the cutting melt flow into the gas steam is written in its boundary layer approximation as follows:

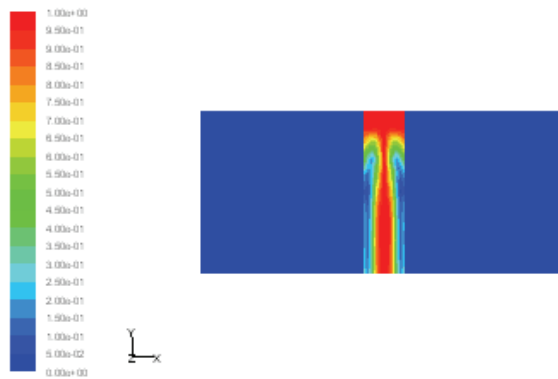
$$\rho C_p \left( u_x \frac{\partial T}{\partial x} + u_y \frac{\partial T}{\partial y} \right) = \frac{\partial}{\partial y} \left( \lambda \frac{\partial T}{\partial y} \right) \quad (5)$$

Where  $C_p$  the specific heat and  $\lambda$  is the thermal conductivity of the molten material. Figure 5 shows for various inert gases the temperature distributions inside the channel at different positions along the y axis: -1.5, -1, -0.5, 0, 1, 1.5 mm.

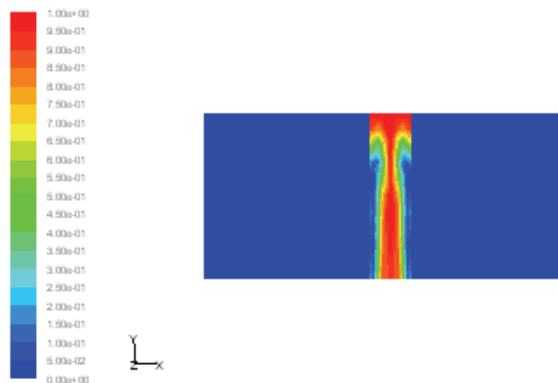
We note that the molten temperature is kept at 1712K, while jet temperature is at 300K. The gas temperature increases particularly in the region close to the walls in the three cases of the inert assist gases. But the heat transfer increases significantly in the middle part of the channel especially for the helium gas (see fig. 5 c); since its thermal conductivity and its specific heat are greater compared to the two others. So, the helium gas reduces the temperature of the melt boundary layer due to the



(a) Argon

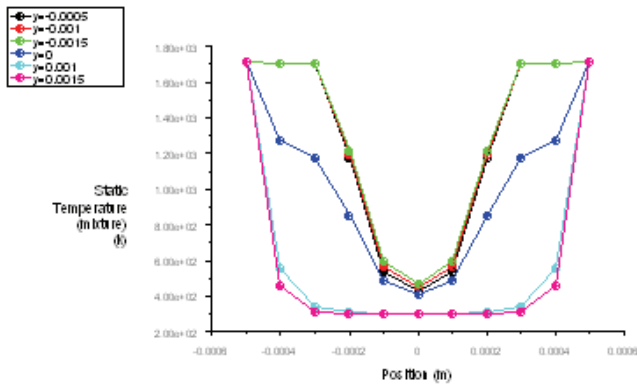


(b) Nitrogen

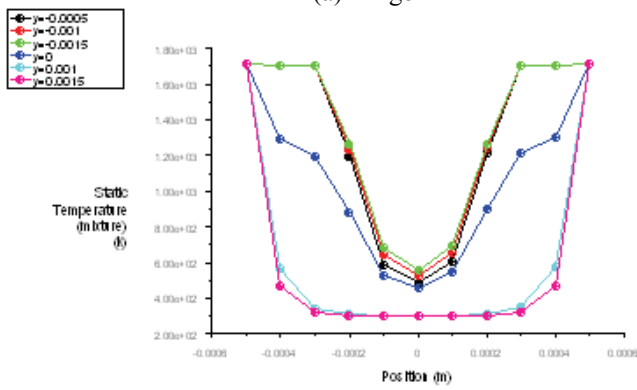


(c) Helium

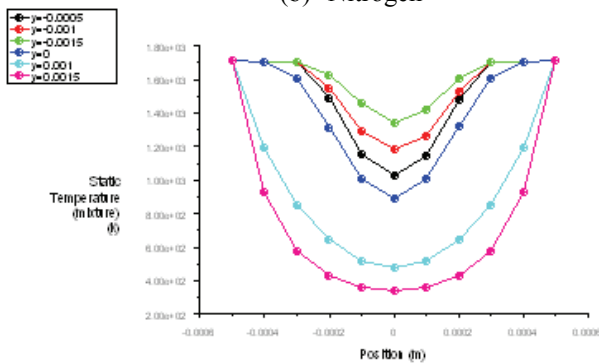
Figure 4: Evacuation of the molten stainless steel with various inert gases



(a) Argon



(b) Nitrogen



(c) Helium

Figure 5: Temperature distribution at different positions inside the channel and for various inert gases.

intense heat transfer in this later case. We note also that the distributions of temperature inside the channel for the nitrogen and argon assist gas are approximately the same.

To understand better what happens, let us calculate the total cooling rate  $Q$  which obeys to the following law [Schlichting (1982)]:

$$Q = kb\Delta T(\rho_g v_g d / \eta)^{0.5} P_r^{\frac{1}{3}} \quad (6)$$

Where  $d$  is the thickness of the workpiece (=4 mm),  $b$  is the space which separates both cutting front (=1 mm),  $\Delta T$  is the temperature difference (i.e., temperature of the molten metal, 1712 K and the temperature of the gas jet, 300K), and  $P_r$  is the Prandtl number.

Knowing that momentum is transferred from the gas jet to the cutting front by a pressure gradient and

friction, so the energy exchange in fusion cutting is mainly due to the heat conduction from the molten material into the gas stream, see tab. 1.

Table 1: Material properties of the used inert gases.

	Nitrogen	Argon	Helium
$\eta$ [kg m <sup>-1</sup> s <sup>-1</sup> ]	1.66 10 <sup>-5</sup>	2.12 10 <sup>-5</sup>	1.99 10 <sup>-5</sup>
$\rho_g$ [kg m <sup>-3</sup> ]	1.138	1.623	0.163
$k$ [Wm <sup>-1</sup> K <sup>-1</sup> ]	0.0242	0.0158	0.152
$C_{pg}$ [J kg <sup>-1</sup> K <sup>-1</sup> ]	1040.7	520.64	5193.0
$Q$ [W]	1.57	1.09	3.45

These calculations show that the helium cools better compared to the two other gases (nitrogen and argon), we have thus more solidification as shown on figure 4 (c). It is clear that the values of the total cooling rates of the argon and nitrogen are close, so the behaviour of the molten stainless steel is approximately the same. The main conclusion is that it is not interesting to use the helium for expelling the molten steel during laser cutting, since it solidifies quickly in a short time compared to the two other gases.

We have also noticed that, these obtained values of the cooling rates, remain negligible compared to the incident laser power generally used in laser cutting which is of typically several kW.

## 4 Conclusion

The energy exchange in pure fusion laser cutting is mainly due to conduction of heat from the molten metal to the gas stream. The vortices that appear during the turbulence observed after the separation point cool the molten metal and extract heat from it. We can thus observe a resolidification of the metal resulting in bad quality of the cutting surface. The stainless steel melt film showed a clear separation point which depends strongly on the gas velocity, but it varies slightly with time and with the nature of the inert gas used. For good cutting quality, a laminar flow regime must be maintained throughout the cut depth to avoid the appearance of the separation point which leads to a turbulent flow and then to a bad quality of cutting. We have also noted that the values of cooling rate obtained for three inert different gases remain negligible near the incident laser power generally required for laser cutting, which is about several kW. Finally, we have concluded that argon and nitrogen are more efficient in laser cutting process of metals since they evacuate more easily the metallic molten film compared to the helium assist gas.

## Nomenclature

$b$	Width of the kerf, [m]
$d$	Thickness of the workpiece, [m]
$C_p$	Specific heat of the molten metal, [ $\text{JKg}^{-1}\text{K}^{-1}$ ]
$k$	Gas conductivity, [ $\text{W K}^{-1}\text{m}^{-1}$ ]
$P$	Gas pressure, [Pa]
$T$	Molten metal temperature, [K]
$t$	Time, [s]
$V$	Velocity of the gas at the entrance, [ $\text{ms}^{-1}$ ]
$u$	Velocity of the molten metal, [ $\text{ms}^{-1}$ ]

## Subscripts

0	At the entrance
$g$	Gas
$x, y$	Cartesian coordinates

## Greek symbols:

$\eta$	Dynamic viscosity of the inert gas, [Pa.s]
$\lambda$	Conductivity of the molten metal, [ $\text{W K}^{-1}\text{m}^{-1}$ ]
$\rho_g$	Density of the inert gas, [ $\text{kg m}^{-3}$ ]

$\mu$	Dynamic viscosity of the molten steel, [ $\text{kg m}^{-1}\text{s}^{-1}$ ]
$\rho$	Density of the molten stainless steel, [ $\text{kg m}^{-3}$ ]
$\delta$	Thickness of the boundary layer, [m]
$\tau$	Shear stress, [ $\text{kg m}^{-1}\text{s}^{-2}$ ]

## References

**Abdulahdi, E.** (1997): Etude de la découpe d'acier au carbone par laser CO<sub>2</sub>. Modélisation thermique et métallurgique du procédé, Thèse d'Etat de l'Ecole Nationale Supérieure des Arts et Métiers.

**Beyer, E.; Himmer, T.; Lütke, M.; Bartels, F.; Mahrle, A.** (2008): Cutting with high brightness lasers, Stuttgart Laser Technologies Forum, Stuttgart, Germany, 4–5 March 2008, German Scientific Society of Laser Technology, Stuttgart.

**Chen, S. L.** (1999): *The effects of high-pressureassistant-gasflowonhigh-powerCO<sub>2</sub> laser cutting.* *Journal of Materials Processing Technology*, vol. 88 pp. 57–66.

**Golnabi, H.; Bahar, M.** (2009): Investigation of optimum condition in oxygen gas assisted laser cutting, *Optics and Laser Technology*, vol. 41, pp. 454-460.

**Hammann, G.** (2008): Laser cutting with CO<sub>2</sub>lasers: The benchmark, Stuttgart Laser Technologies Forum, Stuttgart, Germany, 4–5 March 2008, German Scientific Society of Laser Technology, Stuttgart.

**Kovalev, O. B.; Yudin, P. V.; Zaitsev, A. V.** (2008): Formation of a vortex flow at the laser cutting of sheet metal with low pressure of assisting gas. *J. Phys. D: Appl.*, vol. 41, 155112.

**Mas, C.; Fabbro, R.; Gouédard, Y.** (2003): Steady-State Laser Cutting Modelling, *Journal of Laser Applications*.

**Patankar, S. V.** (1980): *Numerical Heat Transfer and Fluid Flow*, Hemisphere, Publ. Comp., New York, USA.

**Schlichting, H.** (1982): *Boundary Layer Theory*, Mc Graw-Hill, 7th Edition.

**Schulz, W.; Becker, D.; Franke, J.; Kemmerling, R.; Herziger, G.** (1993): Heat conduction losses in laser cutting of metals, *Journal of Physics D: Applied Physics*, vol. 26, pp. 1357-1363.

**Schulz, W.; Kostykin, V.; Nießen, M.; Michel, J.; Petring, D.; Kreutz, E. W.; Poprawe, R.** (1999): Dynamics of ripple formation and melt flow in laser beam cutting, *J. Phys. D*, vol. 32, pp. 1219–1228.

**Tani, G.; Tomesani, L.; Campana, G.** (2003): Prediction of melt geometry in laser cutting, *Applied Surface Science*, vol. 208-209, pp. 142-147.

**Vicanek, M.; Simon, G.** (1987): Momentum and heat transfer of an inert gas jet to the melt in laser cutting, *J. Phys. D*, vol. 20, pp 1191–1196.

**Yilbas, B.S.; Sahin, A.Z.** (1995): Oxygen Assisted Laser Cutting Mechanism-a Laminar Boundary Layer Approach Including the Combustion Process. *Optics and Laser Technology*, vol. 27, no. 3, pp. 175-184.

